Dual-Transmission-Line Microstrip Equiripple Lowpass Filter with Sharp Roll-Off

Vamsi Krishna Velidi and Subrata Sanyal

A novel application of a dual-transmission line is proposed to design a lowpass filter (LPF). The proposed structure uses only transmission line elements to produce an equiripple LPF response with sharp roll-off. Design equations are derived using a lossless transmission line model. Controlling the electrical lengths, three transmission-zeros are realized in the stopband to obtain a sharp roll-off rate and wide stopband bandwidth. A single unit microstrip LPF with a 3-dB cut-off frequency at 1.0 GHz having a roll-off of 135 dB/GHz along with a stopband bandwidth of 69.5% is designed for validation.

Keywords: Lowpass filter, microstrip, transmission line.

I. Introduction

Radio frequency (RF) and microwave wireless applications demand sharp-rejection compact planar lowpass filters (LPFs), for suppression of noise and interference. Conventional transmission-line-based LPFs using open-stubs and stepped-impedance lines have gradual cut-off attenuation characteristics and a narrow upper stopband [1]. Sharp-rejection achieved by increasing the filter order results in increased filter size and insertion loss. Addressing these issues, several methods using ground plane structures [2]-[4], hairpin resonators [5], a patch resonator [6], and coupled hairpin units [7], [8] are proposed to achieve LPFs with sharp cut-off and wide stopband characteristics. Though a wide stopband is achieved, the roll-off rates are 24.3 dB/GHz and 39.1 dB/GHz in [7] and [8], respectively.

Here, a novel application of dual-transmission-line (DTL) topology [9] is proposed to design an equiripple LPF with three attenuation poles in the stopband. A DTL, equivalent to a conventional quarter-wavelength transmission line, is examined for transmission zeros. The proposed configuration involves only transmission line elements and allows the flexibility of using circuit theory approach to design the LPF for different bands and technologies.

II. Analysis of Dual-Transmission Line

Figure 1 shows the proposed DTL configuration equivalent to a conventional transmission line. The topology consists of two dissimilar transmission lines, (Z_1, θ_1) and (Z_2, θ_2), connected in parallel. On equating their Y-parameters, the equivalence between the DTL and a transmission line (Z, θ) is obtained as

$$Z_1 = \frac{Z \sin\theta (\cos\theta_1 - \cos\theta_2)}{\sin\theta_1 (\cos\theta - \cos\theta_2)}, \quad Z_2 = \frac{Z \sin\theta (\cos\theta_2 - \cos\theta_1)}{\sin\theta_2 (\cos\theta - \cos\theta_1)}, \tag{1}$$

$$\frac{Z_2}{Z_1} = \frac{-\sin\theta_1 (\cos\theta - \cos\theta_2)}{\sin\theta_2 (\cos\theta - \cos\theta_1)}. \tag{2}$$

When $\theta = 90°$ (quarter-wavelength) in (2), θ_1 and θ_2 are related by

$$\theta_1 = -\tan^{-1}(K \tan\theta_2), \text{ where } K = Z_2/Z_1. \tag{3}$$

When $K = 1$ for simplicity, the general solution for (2) is

$$\theta_2 = n\pi - \theta_1, \text{ where } n = 1, 2, 3, \ldots \tag{4}$$

Substituting (4) in (1) with $n = 1$ yields

$$Z_1 = Z_2 = 2Z \csc\theta_1. \tag{5}$$

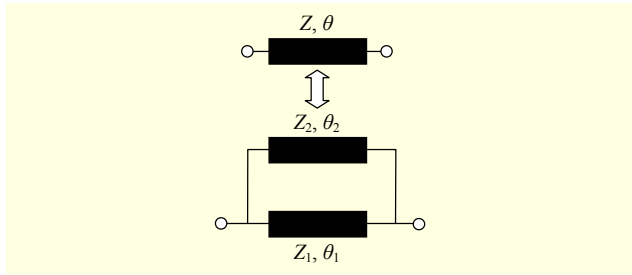The transmission coefficient of the DTL topology with $K = 1$ is

Fig. 1. Topology of DTL equivalent to single transmission line.

Table 1. Impedance solutions for $Z=50\ \Omega$.

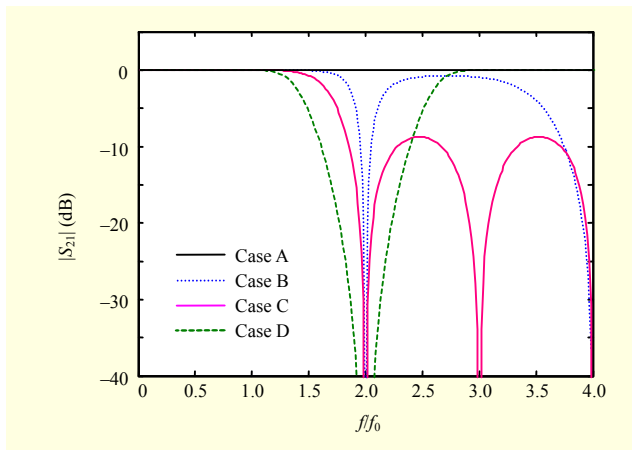| Case	θ_1 (deg.)	$\theta_2 = \pi - \theta_1$ (deg.)	θ_2/θ_1	$Z_1=Z_2$ (Ω)
A	90	90	1.0	100.0
B	72	108	1.5	105.2
C	60	120	2.0	115.5
D	45	135	3.0	141.4
E	30	150	5.0	200.0

Fig. 2. Frequency response of structure for cases in Table 1.

derived as

$$S_{21} = \frac{-j2Z_0 Z_1 P}{Z_1^2 \sin\theta_1 \sin\theta_2 + 2Z_0^2 \left[1 - \cos(\theta_1 + \theta_2)\right] - j2Z_0 Z_1 Q},$$

(6)

where $P = (\sin\theta_1 + \sin\theta_2)$ and $Q = \sin(\theta_1 + \theta_2)$.

With $Z=50\ \Omega$, for different electrical lengths, the impedances satisfying (5) are shown in Table 1. The value of Z_1 or Z_2 increases with increasing electrical length ratio (θ_2/θ_1). For each case, the corresponding filter frequency response (6) normalized to operating frequency (f_0) is plotted in Fig. 2. In case A, the DTL exhibits an allpass response that is identical with that of a conventional line. In contrast, for cases B to E, the responses are lowpass with a passband covering f_0. The
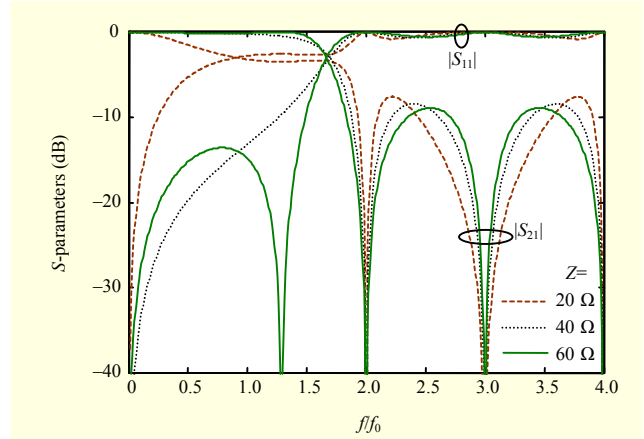

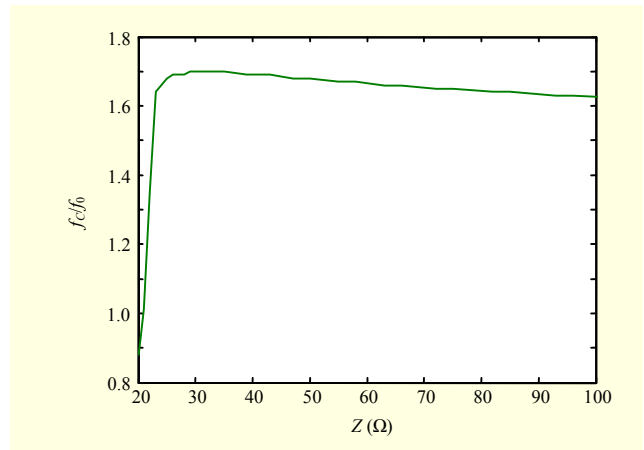Fig. 3. Computed responses of DTL ($\theta_1=\theta_2/2=\pi/3$) for various Z.

Fig. 4. Variation of DTL normalized 3-dB cut-off frequency with Z.

3-dB cutoff frequency shifts down with decreasing (increasing) θ_1 (θ_2). The number of transmission zeros is one (two) in case D (case B) with a narrower stopband bandwidth. In case C, where $\theta_2/\theta_1=2$, three transmission zeros at kf_0 ($k=2, 3, 4$) in the stopband are obtained. This results in a lowpass response with a wide stopband bandwidth. In this case, the fractional bandwidth of separation between first and third zeros is 66.66%.

For case C, the normalized frequency responses of the DTLs, equivalent to $Z=20$-Ω, 40-Ω, and 60-Ω conventional lines, are respectively plotted in Fig. 3. The corresponding impedances for the DTL are $Z_1=46.2\ \Omega$, 92.4 Ω, and 138.6 Ω, respectively. The LPF performance improves with increasing Z (for $Z>20\ \Omega$). Next, the variation of the 3-dB cut-off frequency (f_C), normalized to f_0, with Z (Z_1) ranging from 20 Ω (46.2 Ω) to 100 Ω (230.9 Ω), is shown in Fig. 4. For 20 $\Omega<Z<$ 30 Ω, f_C/f_0 increases from 0.88 to 1.7, and the filter passband response is poor. For $Z>30\ \Omega$, the variation in f_C/f_0 is small (between 1.70 to 1.63), while the filter selectivity increases with increasing Z.

For a wide stopband bandwidth, the minimum stopband

rejection level of the DTL is only −10 dB. On connecting, shunt open-stubs (Z_S, θ_S) at the feed points, as shown in Fig. 5, result in improved stopband rejection level, passband return loss, and filter skirt selectivity. Further, the transmission zeros of the basic DTL are almost not affected by stubs having electrical lengths such that $\pi/8<\theta_S<\pi/4$. If the stub lengths are unequally tuned to produce transmission zeros at $2.5f_0$ ($\theta_S=\pi/5$ at f_0) and $3.5f_0$ ($\theta_S=\pi/5$ at f_0), respectively, then a total of five transmission zeros is produced in the stopband. However, the
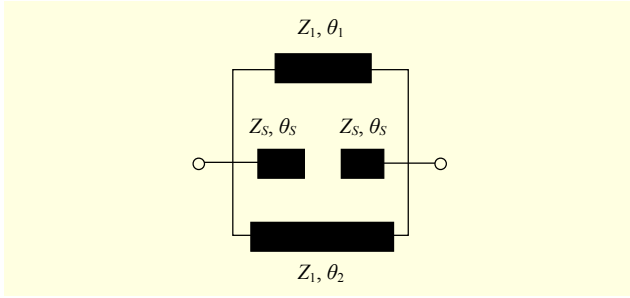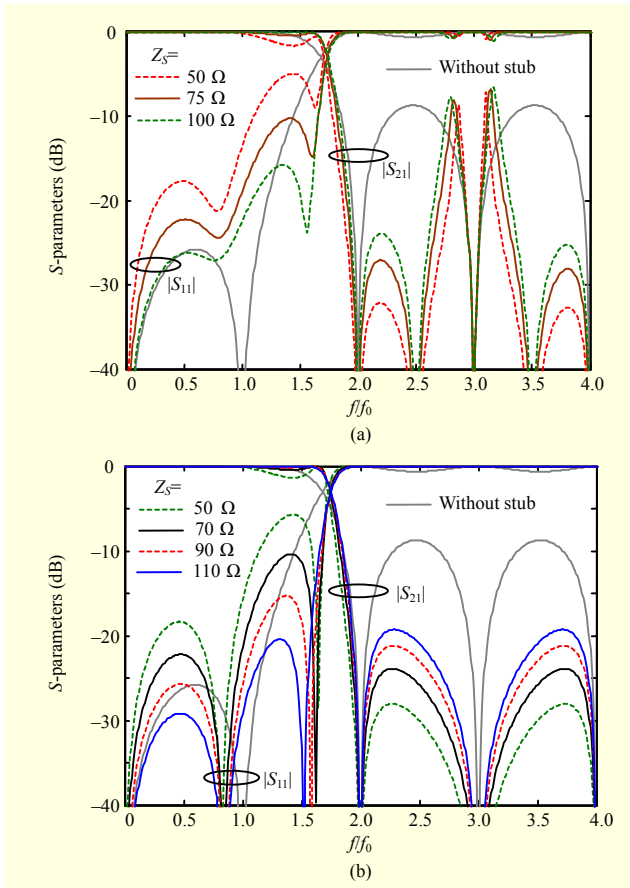
resulting stopband response is not equiripple as two peaks rising beyond −10 dB appear (see Fig. 6(a)). In contrast, if the stubs are equal in length with $\theta_S=\pi/6$ at f_0, the transmission zeros are only at $3f_0$, then the stopband response is equiripple and the rejection depth is high. Figure 6(b) shows the LPF responses for stub impedances Z_S=50 Ω, 70 Ω, 90 Ω, and 110 Ω. The stopband rejection depth increases with decreasing Z_S at the cost of increased return loss in the passband. At better than 20 dB, equal-ripple return loss and insertion loss responses are achieved by optimizing Z_S and Z_1.

III. Measured Results and Discussion

A microstrip LPF having f_C at 1.0 GHz is designed on a 1.58-mm thick FR4 substrate with ε_r=4.3 and $\tan\delta$=0.022. The electrical lengths are $\theta_1=\theta_2/2=2\theta_S=\pi/3$, chosen at f_0=0.57 GHz, so that the LPF has f_C at 1.0 GHz. To begin with, using Fig. 6, where $Z_1=Z_2$=115.5 Ω, Z_S is selected between 90 Ω to 110 Ω for a return loss better than 20 dB. However, the return loss response is not equiripple at this stage. To obtain the equiripple response, the stub impedance and the DTL impedances are now optimized to Z_S=96 Ω and $Z_1=Z_2$=108.5 Ω, respectively. To obtain the physical dimensions of the circuit in the microstrip line, a fullwave electromagnetic simulator IE3D is used. The microstrip layout of the LPF is shown in Fig. 7, where the transmission line sections and the stubs are meandered to achieve an optimally compact geometry. The filter occupies a compact size of 30.6 mm × 36.6 mm ($0.1848\lambda_g \times 0.2210\lambda_g$, where λ_g is the guided wavelength at f_C). Figure 8 illustrates the photograph of the proposed LPF. Measurements are carried out using an Agilent's 8510C vector network analyzer.

Figure 9 compares the circuit predicted, fullwave simulated, and measured frequency responses of the proposed LPF. The measured 3-dB cut-off frequency is 1.036 GHz. The measured insertion loss in the passband is less than 0.5 dB up to 0.766 GHz, while the return loss is better than 18.7 dB throughout the passband. The stopband attenuation is better


Fig. 5. Modified LPF configuration using DTL and open-stubs.

Fig. 6. LPF performances with shunt-open stub impedance Z_S when Z=50 Ω ($Z_1=Z_2$=115.5 Ω and $\theta_1=\theta_2/2=\pi/3$) for (a) unequal length stubs tuned at $2.5f_0$ and $3.5f_0$ and (b) equal-length stubs tuned at $3f_0$.
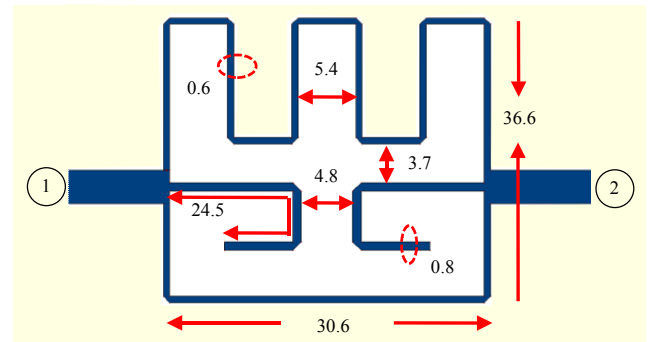

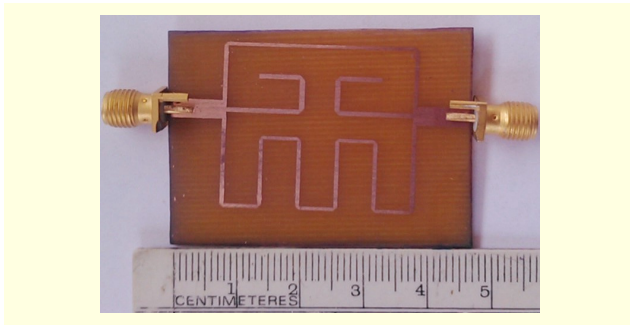Fig. 7. Microstrip layout of the proposed LPF (unit: mm).
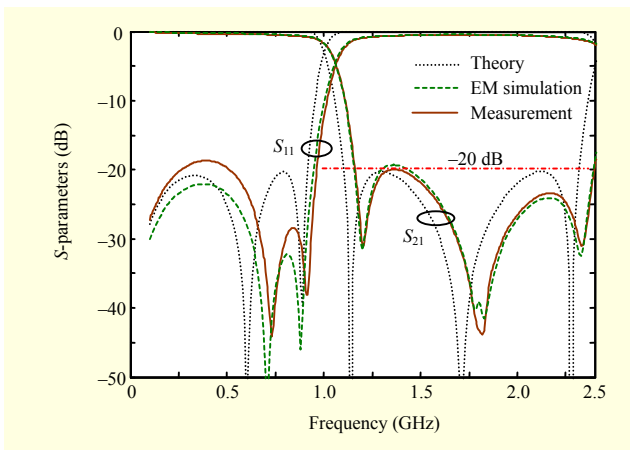
Fig. 8. Photograph of fabricated LPF.

Fig. 9. Measured and simulated responses of proposed LPF.

Table 2. Performance comparison with published LPFs.

	[2]	[3]	[4]	[5]	[6]	This work
f_C (GHz)	2.5	2.4	1.5	1.89	2.4	1.0
Passband RL (dB) IL (dB)	>10 <3.1	>15 <0.3	>17 <0.7	>20 <0.35	>10 NA	>20 <0.5
Stopband rej. (dB)	>40	20	20	20	30	20
Ckt. size (Norm.)	0.23 × 0.17	0.25 × 0.19	NA (large)	0.23 × 0.09	0.35 × 0.11	0.22 × 0.18
Roll-off (dB/GHz)	56	31	43	111	92.5	135
Structure	Double side	Double side	Single side	Double side	Single side	Single side

RL=return loss; IL=insertion loss; Ckt.=circuit; Norm.=normalized to f_C

comparable to those in [2], [3] and more compact than the other LPFs except [4]. Being a double-sided design, the LPF in [4], however, requires a minimum air space volume beneath the ground plane for the structure to be effective. The proposed LPF exhibits good return loss and the highest roll-off rate among the reported filters.

IV. Conclusion

A novel application of dual-transmission lines was presented to design a sharp-rejection lowpass filter. A prototype filter having a 3-dB cut-off frequency f_C at 1.0 GHz and approximately 70% 20-dB rejection bandwidth (up to $2.4f_C$) is fabricated in a microstrip line. The rectangular area of the filter is $0.18\lambda_g \times 0.22\lambda_g$ (λ_g is the guided wavelength of a 50-Ω line at f_C). The filter also shows sharp skirt selectivity with a 135 dB/GHz roll-off rate. The design is flexible and easy to fabricate.

References

[1] D.M. Pozar, *Microwave Engineering*, 2nd ed. New York: Wiley, 1998.

[2] S. Dwari et al., "Compact Wide Stopband Lowpass Filter Using Rectangular Patch Compact Microstrip Resonant Cell and Defected Ground Structure," *Microw. Optical Tech. Lett.*, vol. 49, no. 4, Apr. 2007, pp. 796-798.

[3] J. Yang et al., "Compact Elliptic-Function Low-Pass Filter Using Defected Ground Structure," *IEEE Microw. Wireless Compon. Lett.*, vol. 18, no. 9, Sept. 2008, pp. 578-580.

[4] M.K. Mandal et al., "Low Insertion-Loss Sharp-Rejection and Compact Microstrip Low-Pass Filters," *IEEE Microw. Wireless Compon. Lett.*, vol. 16, no. 11, Nov. 2006, pp. 600-602.

[5] W.-H. Tu et al., "Compact Microstrip Lowpass Filters with Sharp Rejection," *IEEE Microw. Wireless Compon. Lett*, vol. 15, no. 6, June 2005, pp. 404-406.

[6] J.-L. Li et al., "Compact Microstrip Lowpass Filter with Sharp Roll-Off and Wide Stopband," *IET Electron. Lett.*, vol. 45, no. 2, Jan. 2009, pp. 110-111.

[7] S. Luo et al., "Stopband Expanded Lowpass Filters Using Microstrip Coupled-Line Hairpin Units," *IEEE Microw. Wireless Compon. Lett.*, vol. 18, no. 8, Aug. 2008, pp. 506-508.

[8] V.K. Velidi et al., "Micorstrip Coupled-Line Lowpass Filter with Wide Stopband for RF/Wireless Systems," *ETRI J.*, vol. 31, no. 3, June 2009, pp. 324-326.

[9] M.K. Mandal and P. Mondal, "Design of Sharp-Rejection, Compact, Wideband Bandstop Filters," *IET Microw. Antennas Propag.*, vol. 2, no. 4, 2008, pp. 389-393.

than 20 dB from 1.16 GHz to 2.4 GHz resulting in a fractional bandwidth of 69.5%. The filter exhibits a sharp 134.9 dB/GHz roll-off with attenuations, 3 dB at 1.036 GHz and 20 dB at 1.162 GHz.

Table 2 compares the proposed LPF with the best reported sharp roll-off LPFs. The size of the proposed LPF is